

Article

Green Synthesis of Immobilized CuO Photocatalyst for Disinfection of Water

Lev Matoh *, Boštjan Žener and Boštjan Genorio 

Faculty of Chemistry and Chemical Technology, University of Ljubljana, Večna pot 113, 1000 Ljubljana, Slovenia
* Correspondence: lev.matoh@fkkt.uni-lj.si

Abstract: A green method for depositing a CuO layer with good adhesion and a large surface area on a support of activated alumina (Al_2O_3) was evaluated. The relatively simple method consists of adsorption of a copper salt on the surface of Al_2O_3 , formation of $\text{Cu}(\text{OH})_2$, and subsequent decomposition of the hydroxide to CuO. The XRD confirmed that the deposited photocatalyst crystallized at low temperatures (80 °C). Furthermore, BET measurements show a surface area of about 90 m^2/g . The large surface area is the result of the speed of the conversion and decomposition reactions. The photokilling properties of the prepared photocatalyst were evaluated using *E. coli* cells and the leaching of copper ions was determined using ICP-MS. The photocatalytic efficiency was also evaluated by the degradation of an organic azo dye. The prepared photocatalyst shows good activity in the purification and disinfection of treated water. The described method is economical, fast, and can be considered green, since the only byproducts are water and NaCl.

Keywords: CuO; disinfection; visible light photocatalyst; Al_2O_3



check for updates

Citation: Matoh, L.; Žener, B.; Genorio, B. Green Synthesis of Immobilized CuO Photocatalyst for Disinfection of Water. *Sustainability* **2022**, *14*, 10581. <https://doi.org/10.3390/su141710581>

Academic Editor: Andreas Angelakis

Received: 29 July 2022

Accepted: 23 August 2022

Published: 25 August 2022

Publisher's Note: MDPI stays neutral with regard to jurisdictional claims in published maps and institutional affiliations.



Copyright: © 2022 by the authors. Licensee MDPI, Basel, Switzerland. This article is an open access article distributed under the terms and conditions of the Creative Commons Attribution (CC BY) license (<https://creativecommons.org/licenses/by/4.0/>).

1. Introduction

Pretreatment and disinfection of drinking water is a necessary and common step to avoid health problems and ensure good water quality. Usually, this is achieved by adding chemicals, such as chlorine, to the treated water. However, this can result in an altered taste and odor of the water and can also cause the formation of chlorinated organic substances [1–3]. Photocatalysis provides an alternative to current pretreatment methods that does not require the addition of chemicals and is easy to implement [4–8].

Recently, much attention has been focused on the preparation of photocatalysts that are active under visible light illumination, where sunlight can be used to activate the photocatalyst [9]. Most work has been done on modifying TiO_2 , the most common photocatalyst, to shift its absorption spectrum into the visible light range [10–14]. However, an alternative is the use of other materials which have the intrinsic ability to absorb visible light photons, such as CuO, MnO_2 , etc. [15–17].

Copper oxide is a p-type semiconductor with a narrow band gap (1.2–1.4 eV) that allows it to absorb most of the light in the visible spectrum ($\lambda < 1000$ nm) [18–20]. It is, therefore, a promising photocatalyst and has received much attention in recent years. Several studies have shown that CuO has bactericidal properties when irradiated with visible light when the particles are suspended in a solution [21,22]. However, these properties deteriorate rapidly when CuO is immobilized on a support and its active surface area decreases. Since charge separation occurs primarily at the electrolyte–semiconductor junction, a large surface area can significantly enhance the photocatalytic activity of copper oxide [18,19].

Various methods of forming CuO have been reported previously using a hot NaOH solution [23], which exhibits photocatalytic and antimicrobial activity, but the surface area is too small to fully realize its potential [24–26]. Other methods for preparing CuO, such as sol-gel, usually require calcination at high temperatures, while the preparation of coating solutions can be complex and time-consuming [18,27–32].

In this paper, a simple and green method for the preparation of CuO on activated alumina (Al_2O_3) using a hot water-based NaOH solution is explored by utilizing the decomposition of $\text{Cu}(\text{OH})_2$ to CuO in a heated solution. The prepared samples were used to study the bactericidal activity against the bacterium *E. coli* in the dark and under visible light. The photocatalytic properties were also studied by the decomposition of an azo dye, Plasmocorinth B.

2. Materials and Methods

2.1. Materials

The materials in this study were as follows: tripton plus (Fluka Analytical); yeast extract (Fluka Analytical); microbiology agar-agar (Merck); LB agar miller (Novagen); NaOH (Merck); CuCl_2 (Aldrich); Al_2O_3 , granular, 6-8 mesh (Aldrich); Plasmocorinth B, 60% (Sigma Aldrich, St. Louis, MO, USA). All the materials were used as received without any further treatment or purification.

2.2. Synthesis

In a typical procedure, the highly porous activated alumina granules (6-8 mesh) were immersed in a saturated CuCl_2 solution for 5 min to allow the copper salt to adsorb onto Al_2O_3 . The granules were then wiped to remove excess solution from the surface and immersed in a heated solution (80 °C) of 1 M NaOH for 3 min. In the final step, the granules were thoroughly washed with deionized water to remove excess NaOH and residual copper salts. They were then dried at 110 °C and then at 150 °C to remove adsorbed water from the surface of CuO as well as the porous Al_2O_3 support, and finally stored in a dry container.

For XRD and BET measurements, CuO powder was prepared by adding 5 mL of CuCl_2 solution (0.05 g/mL) dropwise to 100 mL of 1 M NaOH heated to 80 °C. The powder was then washed thoroughly with deionized water and dried in air at 110 °C.

2.3. Characterization

The surface morphology of the prepared samples before and after photocatalytic testing were examined using field-emission scanning electron microscopy (FE-SEM, FEI InspectTM F50 and Ultra Plus Zeiss) operated at 2 kV.

The XRD pattern of the powder was obtained using a PANalytical X'Pert PRO MPD instrument in the 2θ range of 5–80° with a step size of 0.034°. The average diameter of crystallites was calculated using the Scherrer equation.

Here, X-ray photoelectron spectroscopy (XPS) measurements were performed using a PHI VersaProbe III (Version AD) (PHI, Chanhassen, MI, USA) equipped with a hemispherical analyzer and a monochromatic Al $K\alpha$ X-ray source. Survey spectra were measured using a pass energy of 224 eV and step of 0.8 eV, while Cu $2p$ core level spectra were measured at a pass energy of 27 eV and step of 0.1 eV. The data were acquired using the ESCApe 1.4 software. Fitting of the Cu $2p$ core level spectra was performed using the CasaXPS 2.3.25 software.

Sync 200 surface area and pore analyzer from 3P Instruments was used to measure the specific surface area (BET). Samples were pre-prepared using a degas procedure with setpoint vacuum (50 mmHg), heated up to 120 °C and held at final conditions for one hour. Samples were analyzed under a nitrogen atmosphere (adsorption desorption isotherms at 77 K) in a volumetric working device. Specific surface areas were calculated using six point values for relative pressures between 0.05 and 0.3.

Then, ICP-MS (Agilent 7500ce ICP-MS) was used to determine the total concentration of copper ions in the bacterial suspension before and after the photo-inactivation tests.

The photokilling activity of the prepared CuO was evaluated as follows. *E. coli* cells (DH5 α strain) were precultured in a 5 mL nutrient broth (LB) for 18 h at 36 °C. The nutrient broth was removed by centrifuging and re-suspending the cells in a 0.9% NaCl solution and diluting it so the final concentration was approximately 10^5 CFU/mL. The suspension was then split into sealed 30 mL transparent plastic containers and one, three, or five granules

with CuO were added to test their effectiveness at inactivating the bacteria. The containers were then stored in the dark or under visible light irradiation (70 W light bulb). After being illuminated for a certain time, samples were aseptically collected, and an appropriate dilution was incubated on an LB agar medium for 24 h at 36 °C to determine the number of viable cells in terms of CFU.

The ability to degrade organic pollutants was evaluated by observing the degradation of Plasmocorinth B (dye concentration = 12 mg/L). The experimental setup was as follows: 10 granules with deposited CuO were dropped into 100 mL of the dye solution and illuminated with a 70 W light bulb. During the reaction the solution was bubbled with oxygen (100 mL/min) to increase the reaction rate and promote the stirring of the solution. Samples were taken every 30 min and the remaining dye concentration was determined by measuring the absorption spectra of the dye in the 400–700 nm range using a Carry 60 UV–Vis spectrophotometer and comparing the absorption values at 550 nm for different samples.

3. Results and Discussion

High surface area CuO with good adhesion formed on the Al₂O₃ support in a two-step solution-based process (Figure 1). In a typical procedure, the first step was the adsorption of the CuCl₂ salt on the surface of Al₂O₃ granules by submerging them in a saturated solution of the copper salt for 5 min. The second step was the formation of Cu(OH)₂ and its decomposition to CuO by dropping the granules with the adsorbed copper salt into a solution of 1 M NaOH, heated to 80 °C, for 3 min. This resulted in the granules turning black, a clear indication that CuO has formed on the surface (Figure 2). The results show that the speed of the reaction was a key factor in obtaining a catalyst with a high surface area and prevented significant degradation of the support, which could slowly dissolve in a high pH solution.

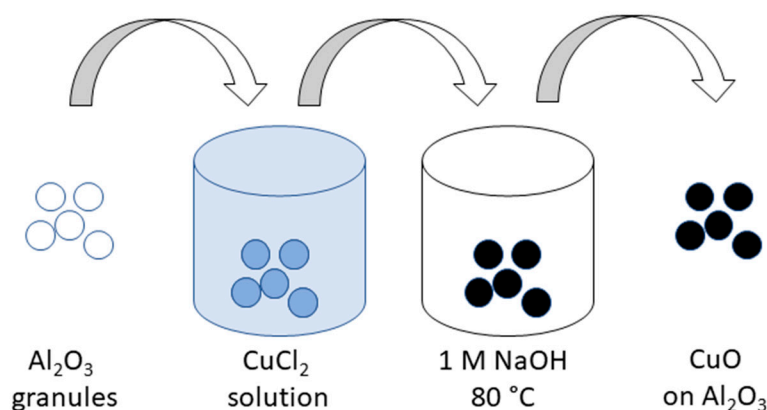


Figure 1. Schematic representation of CuO preparation.



Figure 2. Different stages of CuO preparation: only Al₂O₃ (white), Al₂O₃ with adsorbed copper salt (blue), and Al₂O₃ with CuO (black).

The standard method of CuO formation would be to expose the granules with the adsorbed copper salt to temperatures higher than 300 °C. However, the resulting layers

obtained with this method are more compact and, therefore, have a much lower surface area. It is also more energy consuming and requires the additional step of calcination.

Another advantage of our method is the ability to uniformly deposit CuO on spherical particles of various sizes or uneven surfaces, which is problematic for most deposition methods like dip-coating, spin-coating, etc. The spherical particles could also be used to produce a photocatalytic reactor similar in design to chromatographic columns.

The method described also has the advantage of being environmentally friendly. No organic solvents are used, the required temperature is low, the solutions can be reused, and the only byproducts are water and NaCl.

3.1. Material Characterization

Scanning electron microscopy was used to study the surface of the deposited CuO, which showed the formation of a nanostructured layer with a high specific surface area (Figure 3). The layer consists of randomly distributed flat plates of about 10 nm thickness. The space between the plates is large enough to allow easy access for the solvent and organic molecules.

When CuO is deposited on Al₂O₃, a uniform layer is formed that completely covers the underlying support (Figure 3). No difference in sample morphology was observed after the granules were used in antibacterial or photocatalytic degradation tests.

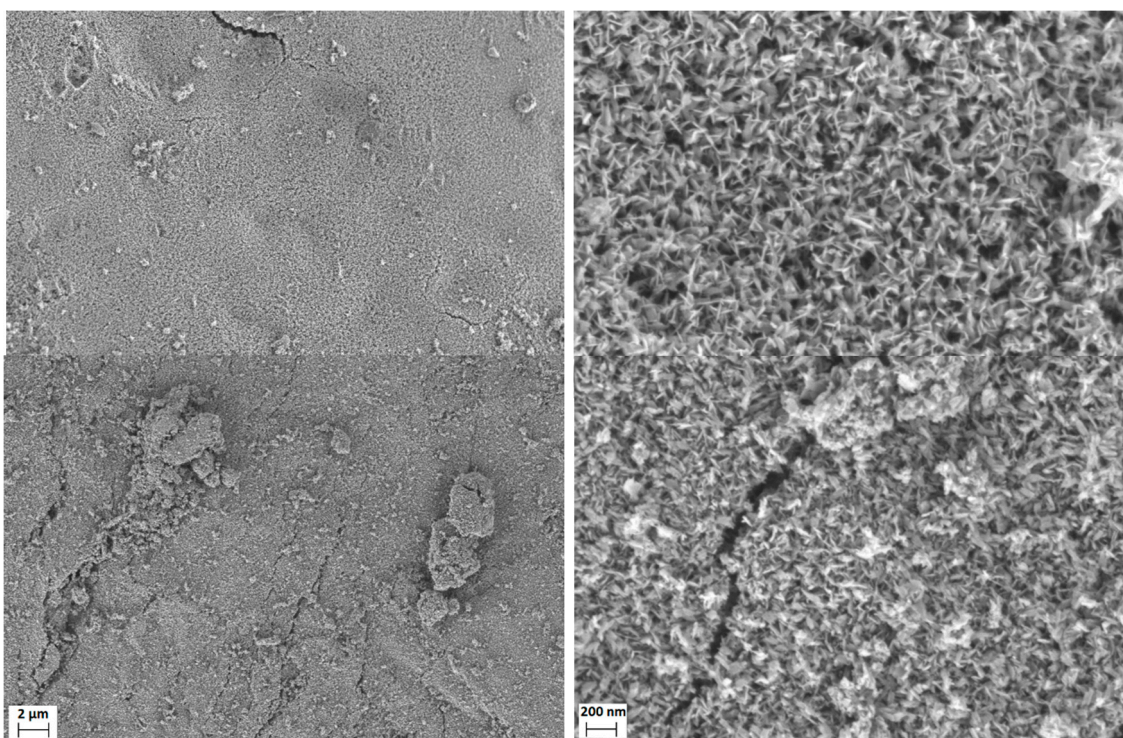


Figure 3. SEM images of CuO on the surface of Al₂O₃ (top) and CuO powder (bottom).

The thickness of the CuO layer covering the outside of Al₂O₃ granules is 0.5–1 μm, but the deposition of the photocatalyst also permeates into the pores a few hundred μm inside the granules (Figure 4). Since there is no clear distinction between layers and the CuO deposits inside the pores are only visible at high magnifications, it is hard to judge the depth using SEM analysis. However, a visual inspection shows an approximately 0.2 mm thick black layer of CuO inside the Al₂O₃ granule (Figure 4).

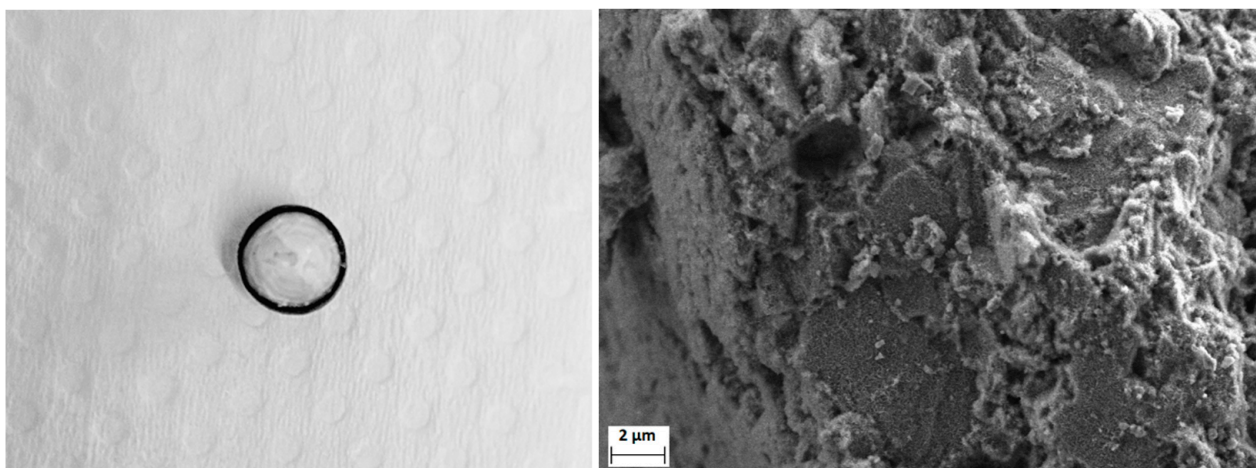


Figure 4. Cross-section of an Al_2O_3 granule with deposited CuO; photograph (left) and SEM image (right).

Because most of the photocatalyst is inside the Al_2O_3 granules, while only a thin layer is present on the surface, its adhesion is excellent and even mechanical forces, such as the ones present during mixing in a solution, do not damage the deposition or cause removal of the photocatalyst. This is also confirmed by ICP-MS (Section 3.3).

Specific area measurements (BET) of the powders show a surface area of approximately $90 \text{ m}^2/\text{g}$ (Figure 5).

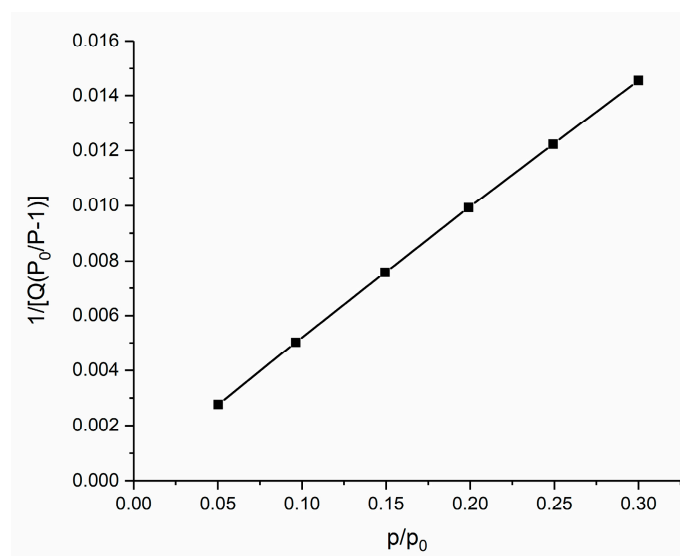


Figure 5. BET surface area plot.

The XRD pattern of the prepared photocatalyst in powder form is shown in Figure 6. All peaks correspond to CuO, and the relative intensity indicates that the sample is in crystalline form. Crystallization was achieved during synthesis at low temperatures ($80 \text{ }^\circ\text{C}$) without additional thermal treatment. The average diameter of the crystallites was calculated using the Scherrer equation and is around 11 nm, which agrees with the results of the SEM analysis.

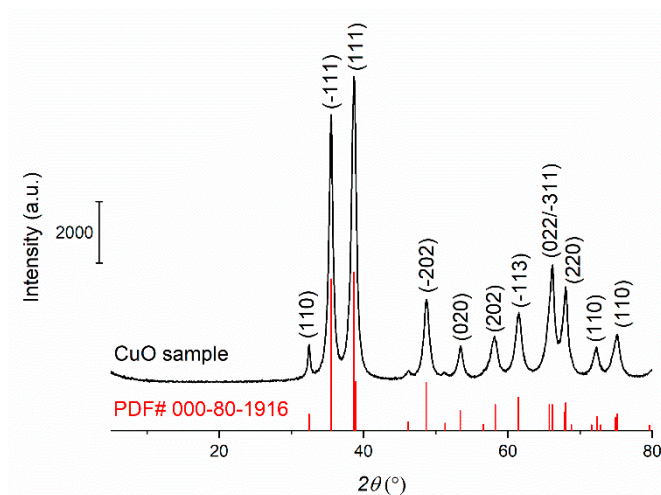


Figure 6. XRD pattern of the prepared CuO powder.

To confirm the presence of Cu^{2+} species, a XPS survey spectrum and a Cu $2p$ core level spectrum were recorded for the CuO sample (Figure 7). Survey spectra (Figure 7a) showed the presence of the expected elements, namely Cu, O, and C. Here, Cu and O are part of the CuO sample while C is adventitious carbon. The Cu $2p_{3/2}$ core level spectrum (Figure 7b) showed $\text{Cu}^{2+} 2p_{1/2}$ and $\text{Cu}^{2+} 2p_{3/2}$ at 953.04 eV and 933.14 eV, respectively. In addition, two shake-up satellites of $\text{Cu}^{2+} 2p_{1/2}$ and $\text{Cu}^{2+} 2p_{3/2}$ were found in the Cu $2p$ spectrum. The spectrum on Figure 7b is consistent with the Cu $2p$ core level spectrum of standard CuO material published previously [33]. The position of the Cu $2p$ core level peaks and the presence of shake-up satellites is a qualitative indication of the presence of Cu^{2+} species used in several publications [33]. However, the Cu $2p_{3/2}$ peak was also fitted using the method described by M. C. Biesinger [33], and the concentration of Cu^{2+} species on the surface of the prepared CuO samples was estimated (Figure S1). Based on the proposed equation, the concentration of Cu^{2+} on the surface of the CuO sample was 88.81 at%. The reason for the presence of low concentrations of Cu^+ and Cu^0 on the surface of the sample is the electron beam induced reduction in CuO described previously [34]. The XPS result are consistent with XRD results and show that Cu^{2+} is prevalent in the CuO sample.

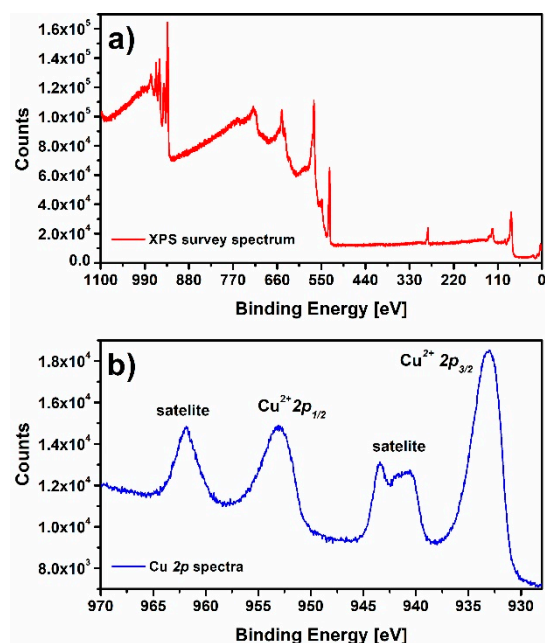


Figure 7. XPS spectra of CuO, (a) XPS survey spectrum, and (b) Cu $2p$ core level spectrum.

3.2. Disinfection Properties

Figure 8 shows the survival percentage of *E. coli* cells in a suspension with CuO-covered Al_2O_3 as a function of time. No changes in survival rate were observed when the sample was stored in the dark or when only Al_2O_3 granules without CuO were used. On the other hand, a sharp decrease in the number of viable cells was observed when the samples containing CuO were illuminated with visible light. This confirms the photocatalytic activity of the prepared samples. Since the samples did not inactivate the bacterial cells in the dark, we can also assume that the leaching of copper ions into the solution did not affect the bacteria or that inactivation occurred by physical damage to the cells upon contact with the sample surface. Cell killing was complete in 90 min regardless of the number of granules used when the initial cell concentration was approximately 10^5 CFU/mL. Although the nano-CuO is attached to a substrate, its surface area appears to be large enough to exhibit photocatalytic ability when illuminated with visible light. The kinetics of bacterial photoinactivation appear to be fairly linear, and no defined stages or lag phases were observed.

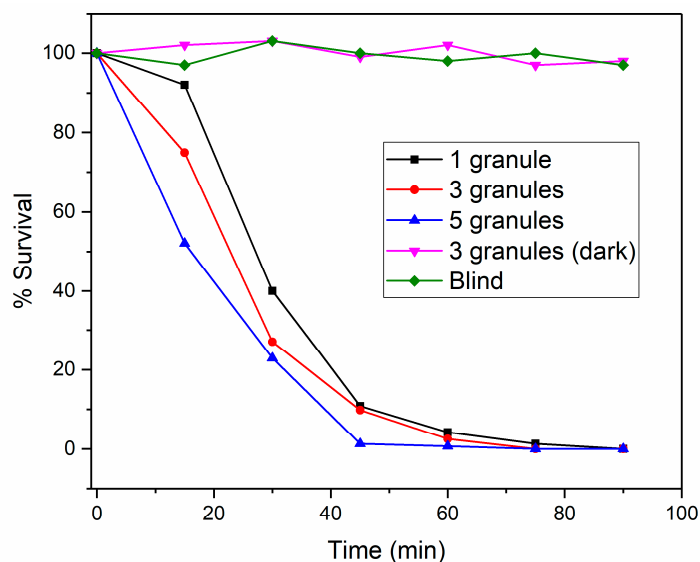


Figure 8. The survival % of *E. coli* bacteria vs. illumination time in the presence of CuO covered Al_2O_3 granules.

The photokilling ability of the samples did not deteriorate even after repeated use (three times), which is consistent with the results of ICP-MS, which showed almost no leaching of copper ions into solution, and SEM, which showed no change in the surface morphology of the samples. However, it is worth noting that, in a more acidic solution, the copper oxide could dissolve almost completely after a short time.

3.3. ICP-MS Measurement

After the antibacterial tests, the total concentration of copper ions in the suspension was determined using ICP-MS. An autoclaved bacterial suspension in 0.9% NaCl served as a blank, the value of which was subtracted from the test results. The resulting copper ion concentration in the solution was less than 0.2 mg/L, indicating that the leaching of copper ions into the solution is minimal and well below the limit for drinking water (1.3–2.0 mg/L) [35,36]. When the CuO samples were stored in an acidic medium, the values determined with ICP-MS for the Cu concentration in the solution were several hundred mg/L.

3.4. Photocatalytic Degradation

To evaluate the photocatalytic ability to degrade organic pollutants, the samples were used to degrade Plasmocorinth B, an organic dye. In Figure 9, the results are divided into two parts. In the first part, adsorption on the surface of the photocatalyst and the underlying alumina support was determined. After 120 min, the light was turned on and photocatalytic degradation began. Because the surface was not yet saturated with the dye, an additional experiment was performed where only adsorption was followed. Comparing the difference in the rate of removal from the solution shows the effect of photocatalytic degradation.

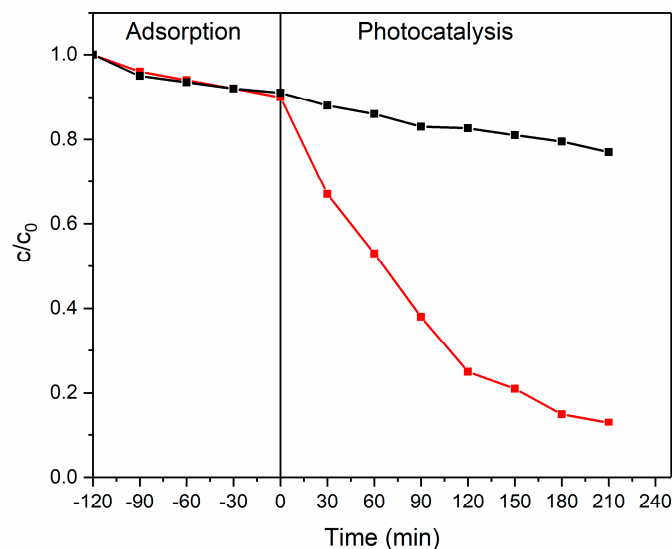


Figure 9. Photocatalytic degradation of Plasmocorinth B using CuO on the Al₂O₃ support (red), and the adsorption of the dye in the dark (black).

4. Conclusions

The prepared nanostructured CuO layer adheres excellently to the Al₂O₃ support and can be effectively used for the disinfection of water or degradation of persistent organic pollutants. The large surface area enables photocatalytic activity under mild environmental conditions, and the alumina support allows quick and easy removal of CuO photocatalyst from the treated water.

Another advantage of the method is that CuO can be easily deposited on spherical granules, and the size of the granules has no effect on the synthesis process. This is in contrast to other deposition methods, such as sol-gel, where uniform deposition on spherical supports is difficult to achieve.

The low leaching of copper ions into the solution and activity under visible light mean that the photocatalyst produced could be used for drinking water disinfection using sunlight, for example in plastic bottles. Furthermore, if smaller granules (<1 mm diameter) are used, a densely packed photocatalytic reactor could be developed.

Supplementary Materials: The following supporting information can be downloaded at: <https://www.mdpi.com/article/10.3390/su141710581/s1>, Figure S1: Cu 2p_{2/3} XPS core level spectra with spectral deconvolution for CuO (red), Cu₂O (blue), and Cu (magenta) species on the surface of the CuO sample.

Author Contributions: Conceptualization, L.M.; methodology, L.M.; investigation, L.M., B.Ž. and B.G.; writing—original draft preparation, L.M.; writing—review and editing, L.M., B.Ž. and B.G. All authors have read and agreed to the published version of the manuscript.

Funding: The authors acknowledge the financial support from the Slovenian Research Agency (research core fundings No. P1-0134, P2-0423 and project L7-1848).

Institutional Review Board Statement: Not applicable.

Informed Consent Statement: Not applicable.

Data Availability Statement: Not applicable.

Conflicts of Interest: The authors declare no conflict of interest.

References

1. Säve-Söderbergh, M.; Toljander, J.; Donat-Vargas, C.; Berglund, M.; Åkesson, A. Exposure to Drinking Water Chlorination By-Products and Fetal Growth and Prematurity: A Nation Wide Register-Based Prospective Study. *Environ. Health Perspect.* **2020**, *128*, 057006. [[CrossRef](#)] [[PubMed](#)]
2. Boorman, G.A.; Dellarco, V.; Dunnick, J.K.; Chapin, R.E.; Hunter, S.; Hauchman, F.; Gardner, H.; Mike, C.; Sills, R.C. Drinking Water Disinfection Byproducts: Review and Approach to Toxicity Evaluation. *Environ. Health Perspect.* **1999**, *107*, 207–217. [[CrossRef](#)] [[PubMed](#)]
3. Richardson, S.D.; Postigo, C. Drinking Water Disinfection By-Products. *Handb. Environ. Chem.* **2012**, *20*, 93–137. [[CrossRef](#)]
4. You, J.; Guo, Y.; Guo, R.; Liu, X. A Review of Visible Light-Active Photocatalysts for Water Disinfection: Features and Prospects. *Chem. Eng. J.* **2019**, *373*, 624–641. [[CrossRef](#)]
5. Sichel, C.; Blanco, J.; Malato, S.; Fernández-Ibáñez, P. Effects of Experimental Conditions on *E.Coli* Survival during Solar Photocatalytic Water Disinfection. *J. Photochem. Photobiol. A Chem.* **2007**, *189*, 239–246. [[CrossRef](#)]
6. Liu, Y.; Zeng, X.; Hu, X.; Hu, J.; Zhang, X. Two-Dimensional Nanomaterials for Photocatalytic Water Disinfection: Recent Progress and Future Challenges. *J. Chem. Technol. Biotechnol.* **2019**, *94*, 22–37. [[CrossRef](#)]
7. Zhang, D.; Li, G.; Yu, J.C. Inorganic Materials for Photocatalytic Water Disinfection. *J. Mater. Chem.* **2010**, *20*, 4529–4536. [[CrossRef](#)]
8. Ahmed, S.N.; Haider, W. Heterogeneous Photocatalysis and Its Potential Applications in Water and Wastewater Treatment: A Review. *Nanotechnology* **2018**, *29*, 342001. [[CrossRef](#)]
9. Djurišić, A.B.; He, Y.; Ng, A.M.C. Visible-Light Photocatalysts: Prospects and Challenges. *APL Mater.* **2020**, *8*, 030903. [[CrossRef](#)]
10. Žener, B.; Matoh, L.; Carraro, G.; Miljević, B.; Korošec, R.C. Sulfur-, Nitrogen- and Platinum-Doped Titania Thin Films with High Catalytic Efficiency under Visible-Light Illumination. *Beilstein J. Nanotechnol.* **2018**, *9*, 1629–1640. [[CrossRef](#)]
11. Anandan, S.; Ikuma, Y.; Niwa, K. An Overview of Semi-Conductor Photocatalysis: Modification of TiO₂ Nanomaterials. *Solid State Phenom.* **2010**, *162*, 239–260. [[CrossRef](#)]
12. Chen, D.; Cheng, Y.; Zhou, N.; Chen, P.; Wang, Y.; Li, K.; Huo, S.; Cheng, P.; Peng, P.; Zhang, R.; et al. Photocatalytic Degradation of Organic Pollutants Using TiO₂-Based Photocatalysts: A Review. *J. Clean. Prod.* **2020**, *268*, 121725. [[CrossRef](#)]
13. Matoh, L.; Žener, B.; Korošec, R.C.; Štangar, U.L. Photocatalytic Water Treatment. In *Nanotechnology in Eco-Efficient Construction*; Pacheco-Torgal, F., Vittoria Diamanti, M., Nazari, A., Goran Granqvist, C., Pruna, A., Amirkhanian, S., Eds.; Elsevier: Duxford, UK, 2019; Volume 4, pp. 675–702, ISBN 9780081026410.
14. Šuligoj, A.; Arčon, I.; Mazaj, M.; Dražič, G.; Arčon, D.; Cool, P.; Štangar, U.L.; Tušar, N.N. Surface Modified Titanium Dioxide Using Transition Metals: Nickel as a Winning Transition Metal for Solar Light Photocatalysis. *J. Mater. Chem. A* **2018**, *6*, 9882–9892. [[CrossRef](#)]
15. Chiam, S.L.; Pung, S.Y.; Yeoh, F.Y. Recent Developments in MnO₂-Based Photocatalysts for Organic Dye Removal: A Review. *Environ. Sci. Pollut. Res.* **2020**, *27*, 5759–5778. [[CrossRef](#)]
16. Rao, M.P.; Sathishkumar, P.; Mangalaraja, R.V.; Asiri, A.M.; Sivashanmugam, P.; Anandan, S. Simple and Low-Cost Synthesis of CuO Nanosheets for Visible-Light-Driven Photocatalytic Degradation of Textile Dyes. *J. Environ. Chem. Eng.* **2018**, *6*, 2003–2010. [[CrossRef](#)]
17. Katal, R.; Masudy-panah, S.; Kong, E.Y.J.; Dasineh Khiavi, N.; Abadi Farahani, M.H.D.; Gong, X. Nanocrystal-Engineered Thin CuO Film Photocatalyst for Visible-Light-Driven Photocatalytic Degradation of Organic Pollutant in Aqueous Solution. *Catal. Today* **2020**, *340*, 236–244. [[CrossRef](#)]
18. Zhang, Q.; Zhang, K.; Xu, D.; Yang, G.; Huang, H.; Nie, F.; Liu, C.; Yang, S. CuO Nanostructures: Synthesis, Characterization, Growth Mechanisms, Fundamental Properties, and Applications. *Prog. Mater. Sci.* **2014**, *60*, 208–337. [[CrossRef](#)]
19. Raizada, P.; Sudhaik, A.; Patial, S.; Hasija, V.; Parwaz Khan, A.A.; Singh, P.; Gautam, S.; Kaur, M.; Nguyen, V.H. Engineering Nanostructures of CuO-Based Photocatalysts for Water Treatment: Current Progress and Future Challenges. *Arab. J. Chem.* **2020**, *13*, 8424–8457. [[CrossRef](#)]
20. Sahu, K.; Choudhary, S.; Khan, S.A.; Pandey, A.; Mohapatra, S. Thermal Evolution of Morphological, Structural, Optical and Photocatalytic Properties of CuO Thin Films. *Nano-Struct. Nano-Objects* **2019**, *17*, 92–102. [[CrossRef](#)]
21. Kumar, K.; Priya, A.; Arun, A.; Hait, S.; Chowdhury, A. Antibacterial and Natural Room-Light Driven Photocatalytic Activities of CuO Nanorods. *Mater. Chem. Phys.* **2019**, *226*, 106–112. [[CrossRef](#)]
22. Momeni, M.M.; Mirhosseini, M.; Nazari, Z.; Kazempour, A.; Hakimiyan, M. Antibacterial and Photocatalytic Activity of CuO Nanostructure Films with Different Morphology. *J. Mater. Sci. Mater. Electron.* **2016**, *27*, 8131–8137. [[CrossRef](#)]
23. Rao, M.P.; Wu, J.J.; Asiri, A.M.; Anandan, S.; Ashokkumar, M. Photocatalytic Properties of Hierarchical CuO Nanosheets Synthesized by a Solution Phase Method. *J. Environ. Sci.* **2018**, *69*, 115–124. [[CrossRef](#)] [[PubMed](#)]

24. Alishah, H.; Pourseyedi, S.; Ebrahimipour, S.Y.; Mahani, S.E.; Rafiei, N. Green Synthesis of Starch-Mediated CuO Nanoparticles: Preparation, Characterization, Antimicrobial Activities and in Vitro MTT Assay against MCF-7 Cell Line. *Rend. Lincei* **2017**, *28*, 65–71. [[CrossRef](#)]
25. Mageshwari, K.; Sathyamoorthy, R. Flower-Shaped CuO Nanostructures: Synthesis, Characterization and Antimicrobial Activity. *J. Mater. Sci. Technol.* **2013**, *29*, 909–914. [[CrossRef](#)]
26. Devi, A.B.; Moirangthem, D.S.; Talukdar, N.C.; Devi, M.D.; Singh, N.R.; Luwang, M.N. Novel Synthesis and Characterization of CuO Nanomaterials: Biological Applications. *Chin. Chem. Lett.* **2014**, *25*, 1615–1619. [[CrossRef](#)]
27. Wang, Y.; Jiang, T.; Meng, D.; Jin, H.; Yu, M. Controllable Fabrication of Nanowire-like CuO Film by Anodization and Its Properties. *Appl. Surf. Sci.* **2015**, *349*, 636–643. [[CrossRef](#)]
28. Dar, M.A.; Nam, S.H.; Kim, Y.S.; Kim, W.B. Synthesis, Characterization, and Electrochemical Properties of Self-Assembled Leaf-like CuO Nanostructures. *J. Solid State Electrochem.* **2010**, *14*, 1719–1726. [[CrossRef](#)]
29. Arshad, A.; Iqbal, J.; Siddiq, M.; Ali, M.U.; Ali, A.; Shabbir, H.; Nazeer, U.B.; Saleem, M.S. Solar Light Triggered Catalytic Performance of Graphene-CuO Nanocomposite for Waste Water Treatment. *Ceram. Int.* **2017**, *43*, 10654–10660. [[CrossRef](#)]
30. Nair, M.T.S.; Guerrero, L.; Arenas, O.L.; Nair, P.K. Chemically Deposited Copper Oxide Thin Films: Structural, Optical and Electrical Characteristics. *Appl. Surf. Sci.* **1999**, *150*, 143–151. [[CrossRef](#)]
31. Filipič, G.; Cvelbar, U. Copper Oxide Nanowires: A Review of Growth. *Nanotechnology* **2012**, *23*, 194001. [[CrossRef](#)]
32. Christy, A.J.; Nehru, L.C.; Umadevi, M. A Novel Combustion Method to Prepare CuO Nanorods and Its Antimicrobial and Photocatalytic Activities. *Powder Technol.* **2013**, *235*, 783–786. [[CrossRef](#)]
33. Biesinger, M.C. Advanced Analysis of Copper X-ray Photoelectron Spectra. *Surf. Interface Anal.* **2017**, *49*, 1325–1334. [[CrossRef](#)]
34. Losev, A.; Rostov, K.; Tyuliev, G. Electron Beam Induced Reduction of CuO in the Presence of a Surface Carbonaceous Layer: An XPS/HREELS Study. *Surf. Sci.* **1989**, *213*, 564–579. [[CrossRef](#)]
35. Fewtrell, L.; Kay, D.; MacGill, S. A Review of the Science behind Drinking Water Standards for Copper. *Int. J. Environ. Health Res.* **2001**, *11*, 161–167. [[CrossRef](#)]
36. World Health Organization & International Programme on Chemical Safety. *Guidelines for Drinking-Water Quality*, 2nd ed.; Health criteria and other supporting information; World Health Organization: Geneva, Switzerland, 1996; Volume 2.